

Kohn effect and the Fermi surface in copper studied by neutron spectroscopy

G. Nilsson and S. Rolandson*

AB Atomenergi, Nyköping, Sweden

(Received 29 June 1973)

The Kohn effect in copper has been investigated at 80 K for selected regions of the phonon dispersion curves, where the effect was believed to be relatively strong, and where good instrumental resolution is obtainable for the neutron spectrometer used. Kohn anomalies are weak in copper, but they can be observed if the measurements are made with due care. About twenty anomalies have been studied and analyzed with the aid of an eighth-nearest-neighbor Born-von Kármán model. The anomalies are interpreted in terms of points on the Fermi surface in the (100) and (110) planes. The representation picture of the Fermi surface thus obtained is in good agreement with those derived from the Haas-van Alphen and magnetoacoustical measurements.

INTRODUCTION

It has been suggested that the Kohn effect may provide a representation of the Fermi surface in the phonon spectra of metals.¹ Thus, the existence of this property has made possible the derivation of the shape of the Fermi surface in aluminium and lead²⁻⁴ from neutron-spectroscopical measurements. Kohn anomalies have also been observed in many other metals (e.g., niobium, molybdenum,⁵ zinc,⁶ but, to our knowledge, observation of the effect has hitherto been restricted to metals with several conduction electrons per atom. Theoretical aspects of the origin, magnitude, and shape of these anomalies have been treated by several authors.⁷⁻¹¹ Even if a consistent theory, which permits calculation from first principles, does not yet exist, the concept whereby observed anomalies are interpreted in terms of points on the Fermi surface is simple enough. Thus, discontinuities in the slope of dispersion curves are expected to occur, at points where the condition

$$\vec{q} + \vec{G} = \vec{K}_2 - \vec{K}_1 \quad (1)$$

is fulfilled. \vec{K}_1 and \vec{K}_2 define two points on the Fermi surface with parallel tangent planes, \vec{G} is any reciprocal-lattice vector, and \vec{q} is a reduced phonon wave vector. Experimental aspects concerning the observation of Kohn anomalies have been discussed by Stedman *et al.*³ and by Weymouth and Stedman.⁴ The relative size of an anomaly is assumed to be

$$S = CMPF(Q)f(\vec{v}_1, \vec{v}_2)/\nu, \quad (2)$$

where C is determined by the local curvature (convex and concave surfaces generate anomalies with opposite signs) and M is a multiplicity factor, which may strengthen an anomaly on account of crystal symmetry. $P = (\vec{Q} \cdot \vec{e}/Q)^2$ is a polarization factor governed by the phonon polarization \vec{e} and

the electron transition $\vec{Q} = \vec{K}_2 - \vec{K}_1$, while ν is the phonon frequency. F is a form factor the uncertainty of whose magnitude has a predominant influence on the theoretical predictions of the value of S . The electron density of states f depends on the

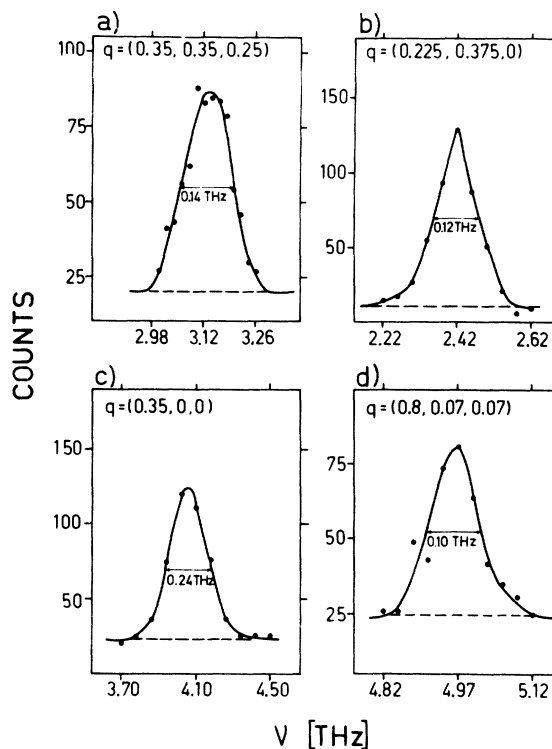


FIG. 1. Some typical phonon peaks recorded in this experiment; (a), (b), and (d) show transverse phonons; (c) longitudinal phonons. These four phonons were measured at the positions of anomalies and are selected from four different series. (In this figure, as well as Figs. 2(b), 3(b), 3(c), 4(a), 4(b), 5(b), and 5(c), the full lines are drawn by inspection and act merely as a guide for the eye.)

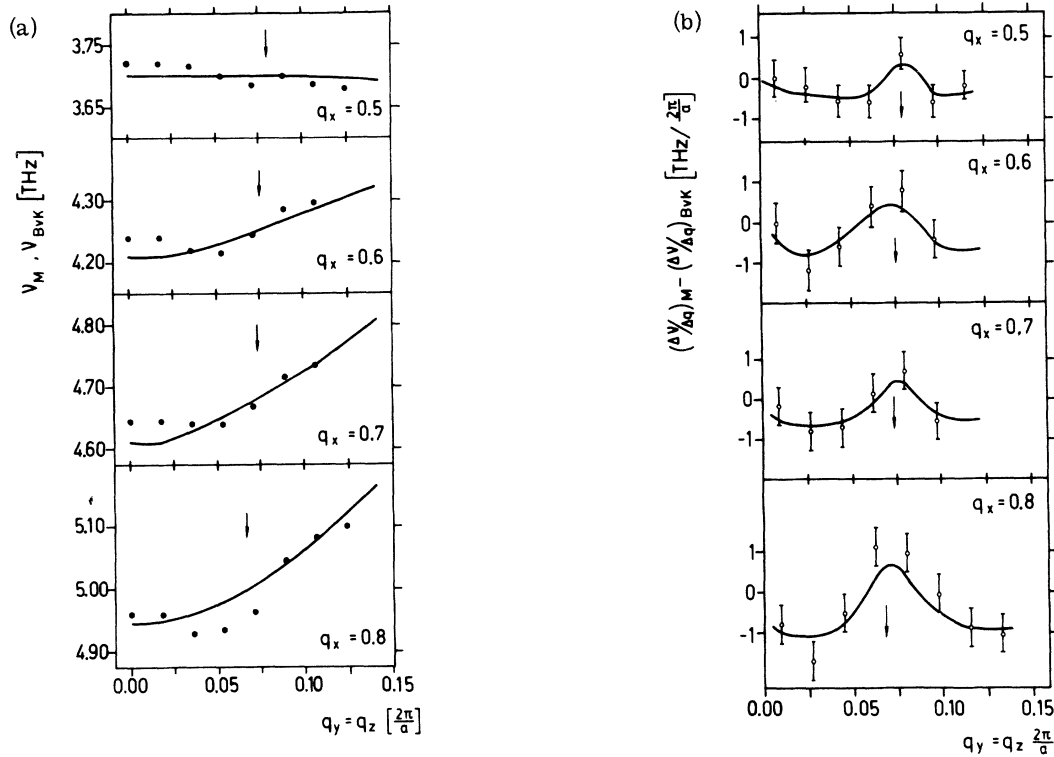


FIG. 2. (a) Four series of transverse phonons measured in the (110) plane parallel to the [110] direction. The magnitude of the estimated errors is given by the size of the dots. In these instances anomalies may be observed in the direct plot of phonon frequencies. Dispersion curves from the Born-von Kármán model are shown for purposes of comparison. (b) Differences between mean slopes from measurements $(\Delta\nu/\Delta q)_M$ and from the model $(\Delta\nu/\Delta q)_{BvK}$ for the curves in (a). Positions of anomalies are indicated by arrows. The outgoing wave vector k_2 was 3.35 \AA^{-1} and the point of observation in reciprocal space \vec{k} was $(q_x, 2 - q_y, 2 - q_z)2\pi/a$.

electron velocities \vec{v}_1 and \vec{v}_2 at the Fermi surface. There is a negative contribution to the phonon frequencies for a convex surface (e.g., a sphere) when $|\vec{q} + \vec{G}| < |\vec{K}_2 - \vec{K}_1|$. This term will disappear when $|\vec{q} + \vec{G}| > |\vec{K}_2 - \vec{K}_1|$. For a concave surface the conditions are reversed while for a saddle surface the situation is more complicated the sign of the contribution depending upon the radii of curvature.³ Weak anomalies are usually studied by plotting the mean slope $(\Delta\nu/\Delta q)$ of the measured dispersion curves as a function of q . This approach renders the kinks more clearly visible for steep curves than does a direct plot of measured phonon frequencies.

The Fermi surface in copper is relatively well known from other kinds of measurements and from theoretical calculations. The main reason for initiating the measurements reported here was to investigate whether the Kohn effect was strong enough to be observed in copper where there is only one conduction electron per atom. Theoreticians have put forward arguments both for and against this possibility. In Taylor's theory the va-

lence, entering as the third power, is the dominant factor which determines the magnitude of the anomalies, and he concludes that the effect in copper is too small to be observable.⁸ On the other hand Vosko *et al.*¹⁰ made extensive calculations of phonon dispersion curves in sodium, aluminium, and lead with one, three, and four conduction electrons per atom, respectively. According to their studies, the relative smallness of Kohn anomalies in sodium depends mainly on the structure (bcc in sodium and fcc in lead, aluminum, and copper) and to a lesser degree on the valence.

In the first search for Kohn anomalies in copper, Svensson *et al.*¹² reported that no such effect could be detected in measurements performed with an accuracy of about 1%. Following a preliminary investigation one of the present authors subsequently reported that the Kohn effect in copper had been observed in measurements with somewhat improved resolution.¹³ The measurements which formed the basis for this conclusion have since been extended and we present here an analysis of the complete data.

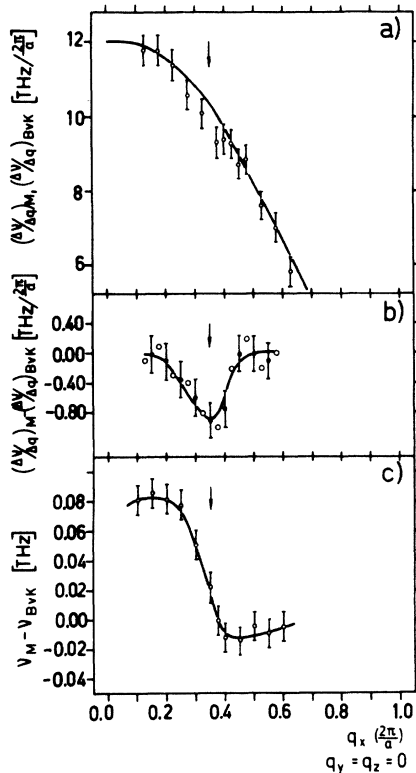


FIG. 3. (a) Mean slopes from measurements $(\Delta\nu/\Delta q)_M$ (dots) and from the model $(\Delta\nu/\Delta q)_{BvK}$ (full lines) for longitudinal phonons in the [100] direction. (b) The differences $(\Delta\nu/\Delta q)_M - (\Delta\nu/\Delta q)_{BvK}$. For filled dots $\Delta q = 0.1$; for open dots $\Delta q = 0.05 (2\pi/a)$. The limits of error for unfilled dots (not shown) is about twice the limits for those which are filled. (c) The difference between measured frequencies ν_M and frequencies from the model ν_{BvK} . These measurements were performed in the (110) plane. $k_2 = 3.25 \text{ \AA}^{-1}$, $\vec{k} = (2 + q_x, 0, 0) 2\pi/a$.

MEASUREMENTS

Regions in reciprocal space where the Kohn effect was expected to produce kinks in the phonon dispersion curves (for diametric electron transitions) were found by constructing diagrams of the Fermi surface at double scale centered at the reciprocal-lattice points. The theoretical results by Segall¹⁴ were used for this purpose. Since in copper the Fermi radius is rather small relative to the dimensions of the Brillouin zone and by comparison with elements possessing several valence electrons, few anomalies were expected to occur in the symmetry directions. It was therefore considered necessary to perform measurements in the off-symmetry directions as well in order to obtain data for a sufficient number of points on the Fermi surface. Series of phonons were measured

at 80 K with small, equally spaced increments in \vec{q} perpendicular to the expected Kohn-anomaly surface using the constant- κ method. Figure 1 shows four typical examples of recorded phonon peaks. The experiment was performed on the same instrument¹⁵ and with techniques similar to those previously used for studies on aluminum² and lead.³ Adequate resolution of energy and momentum was achieved in the instrument by the consistent use of focusing¹⁶ and narrow collimation. Thus the calculated energy resolution was 0.05–0.15 THz, depending on the specific phonon, and the estimated momentum resolution was $(0.02-0.04)(2\pi/a)$ [full-width at half-maximum (FWHM)]. In neutron spectrometry there are many factors, which may disturb the results of single-crystal measurements¹⁷ and they were considered carefully in this investigation.

In order to reveal possible spurious anomalies many series of phonons were recorded two or three times for different analyzer angles or at different positions in reciprocal space. The positions of the phonon peaks and the corresponding errors were then determined by a method described by Stedman and Weymouth.¹⁸ The results of these measurements generally exhibited a high degree of consistency. The angle of the analyzer was fixed during peak scanning. Where possible the monochromator swept through the same angular range for every phonon in a series. Measurements were performed in the (100) and (110) planes in order to study the possibility of determining the points at which the Fermi surface intersect these planes. More than twenty different series with observed anomalies have been measured and about 300 phonon peaks were recorded in this investigation. The measurements were performed in connection with a study of the lattice dynamics in copper, which has been presented elsewhere.¹⁹

For the examples shown in Figs. 2–5 the horizontal collimation before the sample was 0.0065 rad and after 0.013 rad. Vertical collimation was twice the horizontal. Cu(220) was used as monochromator and analyzer. The mosaic width was 0.004 rad for both these crystals. For the sample it was less than 0.002 rad (FWHM). All phonons were recorded with fixed outgoing wave vector and neutron energy loss. The magnitude of the outgoing wave vectors (\vec{k}_2) and the points in reciprocal space (\vec{k}) are given in the figure captions.

ANALYSIS AND RESULTS

Only in a few cases were the phonon curves flat enough to reveal eventual anomalies in a direct plot of phonon frequencies. Figure 2(a) shows examples of the results for measurements obtained for transverse phonons parallel to the [110] direc-

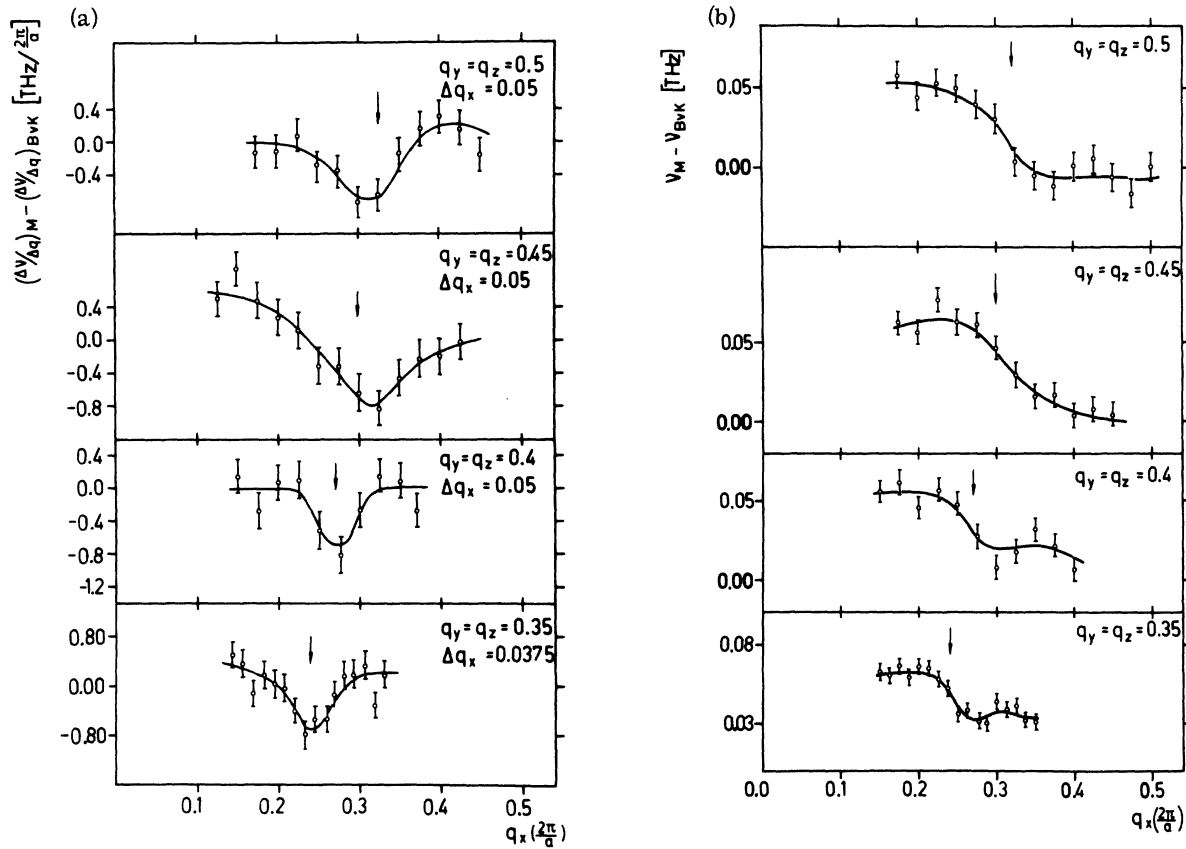


FIG. 4. (a) Differences in slope between the measurements and the model for four series of transverse phonons measured in the (110) plane on lines parallel to the [100] direction. (b) The difference between measurements and the model $\nu_M - \nu_{BvK}$ for the same series of phonons as in (a). $k_2 = 3.5 \text{ \AA}^{-1}$, $\vec{k} = (3 + q_x, 1 - q_y, 1 - q_z) 2\pi/a$.

tion in the (110) plane. Here kinks may be observed at the positions indicated by arrows. It is customary, however, to plot the mean slopes $\Delta v / \Delta q$ in order to render such anomalies observable. In this event it becomes necessary to make a careful choice of Δq since small values increase the limits of error while large values tend to smooth out the anomalies. In the present investigation Δq has been chosen in the range 0.025–0.100, measured in units of $2\pi/a$.

Even when the results are plotted as slopes $(\Delta v / \Delta q)_M$ of the measured dispersion curves, doubt may sometimes arise concerning the assignment of the position and type (positive or negative) of the observed anomalies. Knowledge of the approximate slope of each curve with the kinks removed is desirable if an accurate analysis is to be performed. Many different possibilities exist for comparing the experimental results with the calculated (theoretical) curves. In this investigation consistent use has been made for this purpose of an eighth-nearest-neighbor Born–von Kármán model

with general forces. The model was derived by a least-squares fit to phonon frequencies determined at 145 wave vectors evenly distributed in an irreducible part of the Brillouin zone in reciprocal space.¹⁹ The average deviation from the experimental frequencies for this model was about 0.6%. It is a well known fact that Kohn anomalies in the dispersion curves are of necessity interpreted in a Born–von Kármán model as originating from interactions between very remote neighbors. Similarly, a short-range model is incapable of providing a good fit with the dispersion curves in the vicinity of an anomaly, generating instead smooth curves without a sudden change of slope at the actual point. This effect has been used by Sharp for analyzing Kohn anomalies in niobium.²⁰ For copper, however, the model was expected to give the mean slopes very accurately on account of its high precision. In Fig. 2(a) the Born–von Kármán frequencies are included for comparison, and in Fig. 2(b) the differences in slope as between experiment and model are presented.

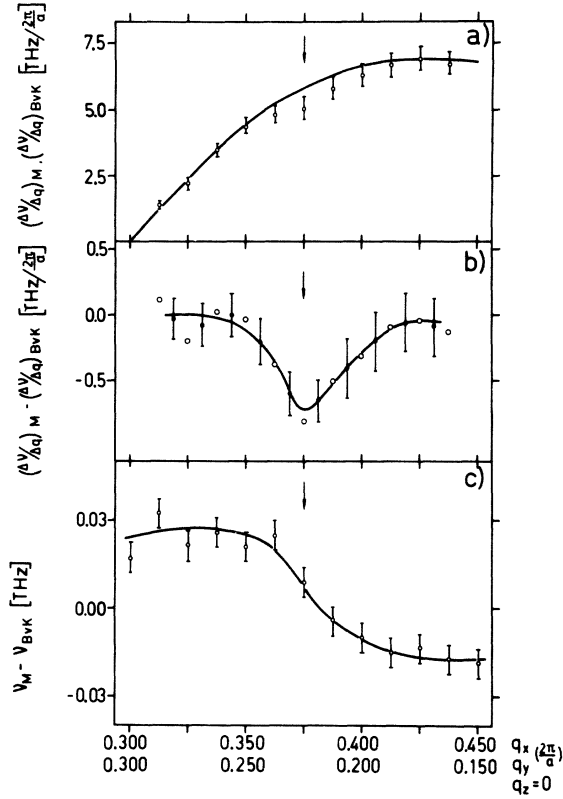


FIG. 5. (a) Slope of a transverse branch of phonons measured in the (100) plane perpendicular to the [110] direction (dots). The slope obtained from the Born-von Kármán model is also shown (full line). (b) The differences between slopes obtained from measurements and from the model. (c) The differences between measured frequencies ν_M and calculated values ν_{BvK} . $k_2 = 3.8 \text{ \AA}^{-1}$, $\bar{k} = (2 + q_x, 2 - q_y, 0) 2\pi/a$.

Analysis of the results was performed by regularly calculating the following quantities for the recorded dispersion curves: (i) the mean slope from measurements $(\Delta\nu/\Delta q)_M$ for constant Δq , (ii) the mean slope $(\Delta\nu/\Delta q)_{\text{BvK}}$ from the Born-von Kármán model for the same values of Δq , (iii) the difference $(\Delta\nu/\Delta q)_M - (\Delta\nu/\Delta q)_{\text{BvK}}$ as a function of q , (iv) the difference between measured frequencies and the corresponding frequencies predicted by the Born-von Kármán model, $\nu_M - \nu_{\text{BvK}}$.

In Fig. 3(a), $(\Delta\nu/\Delta q)_M$ and $(\Delta\nu/\Delta q)_{\text{BvK}}$ are shown for longitudinal phonons in the [100] direction. The differences $(\Delta\nu/\Delta q)_M - (\Delta\nu/\Delta q)_{\text{BvK}}$ and $\nu_M - \nu_{\text{BvK}}$ can be seen in Figs. 3(b) and 3(c), respectively. It would seem that the position of an anomaly is most accurately obtained from a plot of the differences in slope, corresponding to Fig. 3(b), while the magnitude of the anomaly is better seen in a plot of $\nu_M - \nu_{\text{BvK}}$, corresponding to Fig. 3(c). In this last

diagram the measured phonon frequencies are presented individually and the scatter of the points indicates whether the assigned errors are realistic or not. The position of the anomaly should be at a point of inflection for a nearly spherical Fermi surface,⁸ and applying this condition to the results displayed in Fig. 3 the anomaly is found to be positioned at $q = (0.35 \pm 0.02)2\pi/a$. The Fermi radius in the [100] direction is then obtained from this value. Plots of the type shown in Fig. 3(a) can be used to check whether the applied model correctly predicts the slope on either side of the kink. In Table I all the points on the Fermi surface obtained in this experiment are represented by their coordinates in the Brillouin zone.

Some results for measurements performed on transverse phonons in the (110) plane on a line parallel to the [100] direction are shown in Figs. 4(a) and 4(b). In the (100) plane measurements were performed in the [110] direction and in a series orthogonal to this direction. These last-named results are shown in Fig. 5. The positions of the anomalies are indicated in the figures by arrows. Measurements were also performed in the $(2\xi, \xi, \xi)$ direction on longitudinal phonons in order to determine the radius of the neck. Because the anomalies involved in this instance are smaller and the peaks observed broader than average, these measurements may be subject to a systematic error arising out of proximity to a reciprocal lattice

TABLE I. Points on the Fermi surface in copper (in units of $2\pi/a$) as obtained from Kohn anomalies.

Nr	$10k_{F,x}$	$10k_{F,y}$	$10k_{F,z}$
1	8.25 ± 0.10	0.00	0.00
2	7.25 ± 0.15	1.77	1.77
3	7.06 ± 0.13	1.98	1.98
4	6.88 ± 0.13	2.23	2.23
5	6.62 ± 0.15	2.48	2.48
6	6.63 ± 0.10	2.72	2.72
7	6.38 ± 0.10	3.01	3.01
8	6.25 ± 0.10	3.24	3.24
9	6.08 ± 0.10	3.50	3.50
10	6.13 ± 0.10	3.71	3.71
11	6.00 ± 0.10	3.89	3.89
12	6.00 ± 0.10	3.96 ± 0.11	3.96 ± 0.11
13	5.93 ± 0.10	4.21	4.21
14	6.00 ± 0.10	4.46	4.46
15	5.94 ± 0.10	4.54	4.54
16	2.75	5.41 ± 0.09	5.41 ± 0.09
17	2.50	5.39 ± 0.09	5.39 ± 0.09
18	2.25	5.36 ± 0.09	5.36 ± 0.09
19	2.00	5.39 ± 0.09	5.39 ± 0.09
20	1.50	5.36 ± 0.09	5.36 ± 0.09
21	1.00	5.36 ± 0.09	5.36 ± 0.09
22	0.00	5.27 ± 0.09	5.27 ± 0.09
23	8.12 ± 0.10	1.12 ± 0.10	0.00
24	7.25 ± 0.20	2.75 ± 0.20	0.00

point.¹⁷ Several series of phonons were measured on two different samples and the mean value of the anomaly is found to lie at $\xi = (0.20 \pm 0.03)2\pi/a$. This position is in accordance with the results from neighboring anomalies measured on transverse branches (see Fig. 6). Perrin *et al.*²¹ have pointed out that the radius of the neck should vary considerably in different directions, the minimum (0.16 free-electron radii) coinciding with the line from L (0.5, 0.5, 0.5) to K (0.75, 0.75, 0) and the maximum (0.21 free-electron radii) with the line from L to W (1.0, 0.5, 0). Such a variation, although not so marked, seems plausible, in view of the experimental results obtained, both with regard to the position and to the sign of these "anomalies"; the limits of error are such, however, as to prevent any definite conclusion being drawn in this respect, and these results are not included in the table or figures. Twenty-three observed anomalies in Fig. 6 are interpreted in terms of points on the Fermi surface and their coordinates are tabulated in Table I. The full line in Fig. 6 represents the Fermi surface in copper obtained in an analysis of de Haas-van Alphen measurements by Zornberg and Mueller.²²

Anomalies with origins other than those discussed above have been suspected in phonon spectra. Thus Maris²³ suggested that anomalies arise from pho-

non-phonon interactions while Harrison²⁴ predicted anomalies that reflect the electron energy-wave-vector dependence. Even if these other effects have not been studied as extensively as the Kohn effect, kinks have been observed which can scarcely be interpreted in terms of Kohn anomalies. Such kinks were reported in studies on lead³ and aluminum.⁴ Even in the present investigation kinks have been observed which defy explanation on the basis of the Kohn effect. Such anomalies were observed on the branch with the lowest frequency in the range $\vec{q} = (0.1-0.3, 0.05, 0.05)2\pi/a$.

The Fermi surface in copper deviates little from the sphere obtained for free electrons, apart from the necks which project in the $[111]$ directions. Nevertheless, the sign of the anomalies shown in Fig. 4 is opposite to that expected for a spherical surface. This is, however, reasonable if the local radius of curvature is taken into consideration; in the (110) plane this is opposite to that of a sphere over an extended region between the $[111]$ and $[100]$ directions. If the assumptions made by Perrin *et al.*, discussed above, are correct the local surface of the neck is concave (in any direction) in the region of its intersection with the (110) plane.

In the present investigation anomalies have been observed in 23 series of measurements, and although they are of small magnitude their direction (positive or negative) is as expected at all points.³ This fact, taken in conjunction with their reasonable position (with the exceptions mentioned above), provides a strong indication that the observed anomalies are of the Kohn type.

Use of the Born-von Kármán model offers an objective method of finding the position, magnitude and sign of these anomalies. The shape or widths of recorded phonon peaks are not noticeably influenced at the kinks. The peaks shown in Fig. 1 were recorded precisely at the position of anomalies, and in the context of this investigation they may be considered as typical phonons.

The Fermi surface in copper has been extensively studied using other methods. Within the limits of error the present results are in agreement with the high-precision analysis of de Haas-van Alphen measurements conducted by Zornberg and Mueller²² and with the magnetoacoustical measurements performed by Kamm.²⁵ Mijnaerends used positron annihilation in order to study the Fermi surface in copper.²⁶ In the $[110]$ direction he obtained a radius which exceeds $K_{f.e.}$ (the radius for free electrons), and which is greater than that obtained employing the other methods considered here. On the other hand Perrin *et al.* used radio-frequency size effects for their study,²¹ and obtained a value of $0.92K_{f.e.}$, which is the smallest to be reported. These results are included for comparison in Fig. 6. Both of these extreme values lie outside the limits of

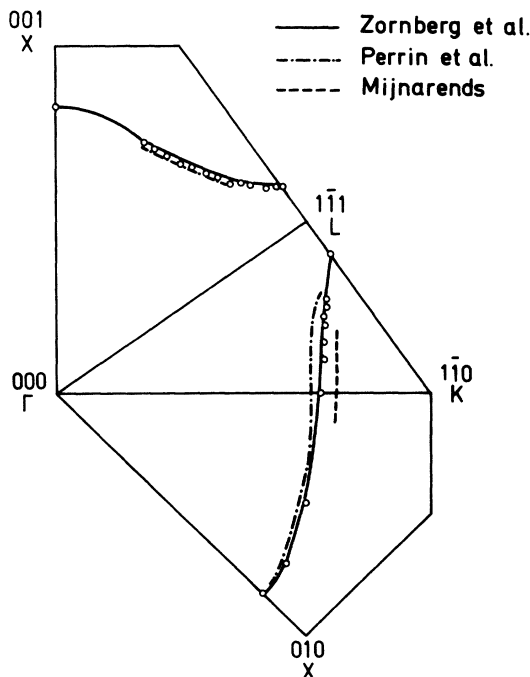


FIG. 6. Anomalies observed in this work interpreted as points on the Fermi surface in the (110) and (100) planes. Comparison with other measurements is made.

error for the measurements presented here. In the vicinity of the anomalies shown in Figs. 4(a) and 4(b) the mean values of the present results lie between those obtained in Refs. 21, 22, and 25, although in general both are covered by the error bars of the individual points. For the measurements in the [100] direction there is satisfactory agreement between all the experimental results considered here.

It was pointed out at an early stage in the investigation of Kohn anomalies that studies of the Fermi surface in metals using the Kohn effect may provide

an effective means of conducting studies in situations where the conventional methods are inapplicable, e.g., at elevated temperatures or in alloys. The present investigation is encouraging in this respect, since even in copper, where the effect is weak in relation to the case in many other metals, the relevant anomalies are observable using fairly conventional methods. Improvements in experimental technique such as can be provided by reactors with stronger flux, should yield further possibilities in the field of Fermi-surface studies using neutron scattering.

*Present address: Pinstech, P. O. Nilore, Rawalpindi, Pakistan.

¹W. Kohn, Phys. Rev. Lett. 2, 393 (1959).

²R. Stedman and G. Nilsson, Phys. Rev. Lett. 15, 634 (1965).

³R. Stedman, L. Almqvist, G. Nilsson, and G. Raunio, Phys. Rev. 163, 567 (1967).

⁴J. Weymouth and R. Stedman, Phys. Rev. B 2, 4743 (1970).

⁵G. Dolling and A. D. B. Woods, in *Thermal Neutron Scattering*, edited by P. A. Egelstaff (Academic, London, 1965), pp. 209–212.

⁶L. Almqvist and R. Stedman, J. Phys. F 1, 785 (1971).

⁷E. J. Woll, Jr. and W. Kohn, Phys. Rev. 126, 1693 (1962).

⁸P. L. Taylor, Phys. Rev. 131, 1995 (1963).

⁹L. M. Roth, H. J. Zeiger, and T. A. Kaplan, Phys. Rev. 149, 519 (1966).

¹⁰S. H. Vosko, R. Taylor, and G. H. Keech, Can. J. Phys. 43, 1187 (1965).

¹¹A. M. Afanasév and Yu. Kagan, Zh. Eksp. Teor. Fiz. 43, 1456 (1962) [Sov. Phys. -JETP 16, 1030 (1963)].

¹²E. C. Svensson, B. N. Brockhouse and J. M. Rowe, Phys. Rev. 155, 619 (1967).

¹³G. Nilsson, in *Neutron Inelastic Scattering, Proceedings of the Symposium, Copenhagen, 1968* (IAEA, Vienna, 1968), Vol. I, p. 187.

¹⁴B. Segall, Phys. Rev. 125, 109 (1962).

¹⁵R. Stedman and G. Nilsson, Rev. Sci. Instrum. 39, 637 (1968).

¹⁶R. Stedman, Rev. Sci. Instrum. 39, 878 (1968).

¹⁷R. Stedman and G. Nilsson, in *Neutron Inelastic Scattering, Proceedings of the Symposium, Bombay, 1964* (IAEA, Vienna, 1965), p. 213.

¹⁸R. Stedman and J. Weymouth, Brit. J. Appl. Phys. 2, 903 (1969).

¹⁹G. Nilsson and S. Rolandson, Phys. Rev. B 7, 2393 (1973).

²⁰R. I. Sharp, J. Phys. C 2, 432 (1969).

²¹B. Perrin, G. Weisbuch, and A. Libchaber, Phys. Rev. B 1, 1501 (1970).

²²E. I. Zornberg and F. M. Mueller, Phys. Rev. 151, 557 (1966).

²³H. J. Maris, Phys. Lett. 22, 402 (1966).

²⁴W. Harrison, Phys. Rev. 129, 2512 (1963).

²⁵G. N. Kamm, Phys. Rev. B 1, 554 (1970).

²⁶P. E. Mijnarends, Phys. Rev. 178, 622 (1969).